HYSHOT-2 AERODYNAMICS

T. Cain, R. Owen and C. Walton

QinetiQ, Room 1079, A7 Building, Cody Technology Park, Ively Road, Farnborough, Hampshire, England, GU14 0LX,
Email: reowen@qinetiq.com

ABSTRACT

The scramjet flight test Hyshot-2, flew on the 30 July 2002. The programme, led by the University of Queensland, had the primary objective of obtaining supersonic combustion data in flight for comparison with measurements made in shock tunnels. QinetiQ was one of the sponsors, and also provided aerodynamic data and trajectory predictions for the ballistic re-entry of the spinning sounding rocket. The unconventional missile geometry created by the nose-mounted asymmetric-scramjet in conjunction with the high angle of attack during re-entry makes the problem interesting. This paper presents the wind tunnel measurements and aerodynamic calculations used as input for the trajectory prediction. Indirect comparison is made with data obtained in the Hyshot-2 flight using a 6 degree-of-freedom trajectory simulation.

1. INTRODUCTION

The Hyshot-2 launch was very close to nominal and supersonic combustion data were obtained from the University of Queensland (UQ) scramjet pictured in Figure 1. The two-stage sounding rocket was launched from a rail at 77° from the horizontal to enable the rocket to accelerate in the upper atmosphere, minimising the energy loss due to drag. The engine remained attached to the Orion second stage for the whole flight and the vehicle is referred to here as the UQ-Orion. A nose cone covered the scramjet during the launch.

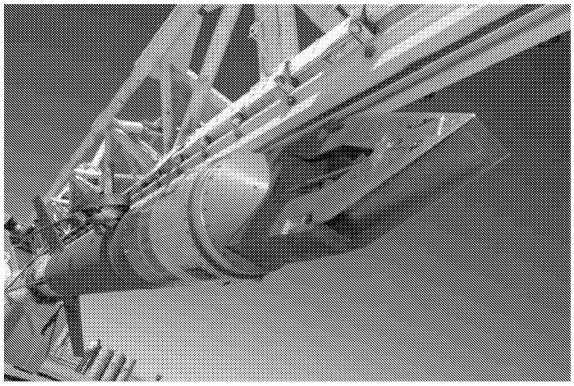

Figure 1 The UQ engine mounted on the Orion.
© 2002 The University of Queensland

A Terrier MK-70 motor was used to boost the UQ-Orion to Mach 3.6 in the first six seconds of the flight. The Orion 5A motor lit at approximately t=15s and continued burning for 25 seconds. The nose cone was ejected at t=64s and an altitude of approximately 107km. A manoeuvre to align the vehicle axis with the re-entry velocity vector began at t=76s and finished at t=201s. The manoeuvre left the vehicle oscillating in a stable coning motion, with 5.6° half-angle and a period of 8.0 seconds. At t=515s the vehicle departed from the stable coning motion as it re-entered the atmosphere and aerodynamic forces increased. The combustion test began at t=537s and telemetry ends at t=545s.

This paper presents a comparison of the measured pitch, angle of attack and axial-magnetometer output during the last 30s of flight with predictions based on aerodynamic coefficients measured in the QinetiQ hypersonic tunnels.

2. OBJECTIVE

Early in the Hyshot programme it became clear that the unusual profile of the UQ engine could make the vehicle unstable. Concerned with the UQ intake's 4° angle-of-attack operational limit, QinetiQ began an investigation of the vehicle aerodynamics and trajectory. Initially, analytical techniques were used to estimate aerodynamic coefficients. The vehicle was predicted to be unstable at small incidence and even at large incidence had a smaller static-margin than had been assumed for the nominal trajectory. Wind tunnel measurements were needed to determine if aerodynamic modifications were necessary and to establish the maximum angle of attack at reentry for which incidence would be below 4° at the scramjet test altitude. UQ were developing a cold-gas thruster system to align the vehicle axis with the reentry velocity vector while in space, and wanted to know maximum allowable misalignment.

3. UQ-ORION

An image from the 3D CAD model that was constructed to determine mass properties is presented in figure 2. The masses of the blocks representing ancillary equipment in the CAD model were adjusted to match the UQ measurements of the payload's mass and centre of gravity. The values for the Orion are as calculated

Proceedings of the Fifth European Symposium on Aerothermodynamics for Space Vehicles, 8-11 November 2005, Cologne, Germany
(ESA SP-563, February 2005)

from the known geometry and are in good agreement with the figures supplied by the launch provider, Defence Technology Industries Inc.

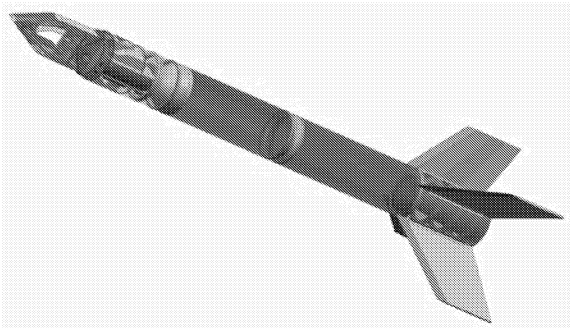

Stage	m, kg	x_{cg}, cm	I_{xx}, kg.m^2	I_{yy}, kg.m^2
Payload	102	74	1.45	10.5
Orion	137	104	5.97	106
CAD Total	239	198	7.4	410
Adopted Total	239	198	8.4	361

Figure 2 Mass properties of the UQ-Orion. x_{cg} is measured from the Orion base, except for the payload for which it is measured from the intake leading edge.

There is a problem with the mass properties as determined by the CAD model in that the ratio I_{yy}/I_{xx} is not correct. While in space the UQ-Orion was coning and its nutation frequency accurately showed the ratio to be 42.7 (Owen and Cain, 2004). To match this value we needed to change I_{xx} or I_{yy} or both. Not knowing why the CAD model was wrong, we distributed the percentage error evenly such that both inertia were adjusted by the factor 1.14. Although this throws some doubt on the accuracy of mass, m, and centre-of-gravity, x_{cg}, presumably the values given for the components are reliable, as they are relatively easy to measure.

4. WIND TUNNELS AND MODELS

Two 7% scale wind tunnel models of the UQ-Orion were tested. UQ1 was made in 1997 while the scramjet was still under development and the second model, UQ2, in 2001 after the Hyshot-1 flight. The latter model is a more faithful representation of the UQ-Orion but was tested only at high Reynolds number. Aerodynamic correlations based on both low and high Reynolds number tests of UQ1 are used to extend the limited data obtained with UQ2.

The UQ-Orion enters the atmosphere at over 2km/s and descends through the full spectrum of flow types from free-molecular to high density continuum. While free-molecular and continuum flow can be modelled reasonably well analytically, the transitional flow between these extremes is more complex. QinetiQ's Low Density Tunnel (LDT) was designed for measurements in the transitional regime. The test gas is nitrogen with a stagnation pressure and temperature of 2.2bar and 1500K respectively. The tunnel runs for periods of up to 30min employing a 45kW graphite heater and up to five 6m^3.s^{-1} roots blowers with associated backing pumps.

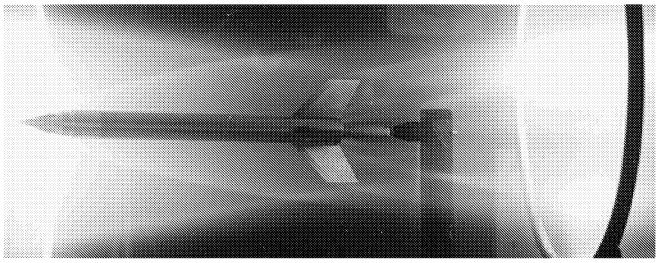

Figure 3 UQ1 at Mach 9.9 in the LDT

A 50Hz 5kV glow discharge system is used for flow visualisation. The rings visible upstream and downstream of the model in figure 3 are connected to the 5kV supply. The Mach 9.9 free-jet flow is from left to right and passes through the rings. The jet is contracting due to high back pressure in the test section but the oblique shocks pass outside the model tail fins (fig 3). The model is mounted on a 3 component force balance that measures pitching moment, and axial and normal forces.

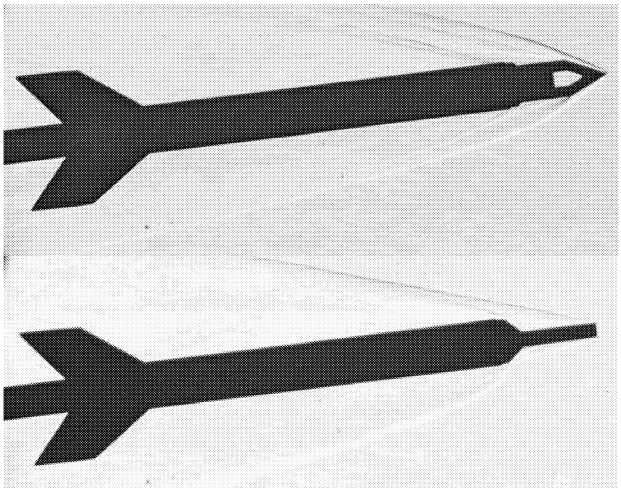

Figure 4 UQ2 at Mach 6.7 in the HDT

Low altitude data were obtained in QinetiQ's High Density Tunnel (HDT). The HDT is an 18m long 152mm diameter electrically heated Ludwieg tube. It has a fast acting valve that opens in approximately 20ms leaving approximately 70ms of steady test time. A conical nozzle with a nominal Mach number of 6.7 was used for these experiments. Figure 4 is composed of schlieren photographs of UQ2 mounted on a 6

component internal force balance. Base pressure was measured with Endevco transducers fixed to the sting. The test conditions are summarised in table 1.

Tunnel	M	Re	$M/\sqrt{Re}$	Kn
HDT	6.7	5.6×10^{5}	9×10^{-3}	1.8×10^{-5}
LDT	9.9	2.3×10^{3}	0.20	6.4×10^{-3}

Table 1 Test conditions with Re based on diameter and $Kn=1.48M/Re$

5. AXIS SYSTEM AND NOTATION

For the trajectory calculation a right-handed body-axes system is defined that has x positive pointing forwards and y positive to starboard. Figure 5 shows a cross sectional view through the UQ-Orion looking forward along the x-axis.

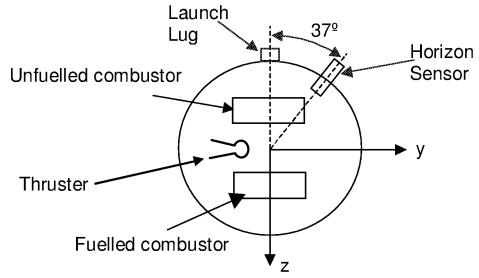

Figure 5 Looking from behind the UQ-Orion

Vehicle orientation is defined by Yaw, ψ, Pitch, θ, and Roll, ϕ. For ease of comparison with the horizon sensor and magnetometer outputs, ψ, θ and ϕ are defined by rotating from an axis system X, Y and Z, the origin of which moves with the vehicle, but where X is due North, Y is due East and Z is vertically down. The body attitude is obtained by first yawing an angle ψ about Z, then pitching θ about y and finally rolling ϕ about x. All rotations are positive clockwise.

For presentation of the aerodynamic data it is more convenient to work with a wind tunnel based axes system. In this system the free stream velocity vector is always in the x, z plane and x is aligned with the vehicle axis and positive rearwards. A positive angle of attack corresponds to a positive rotation about y. Moments about x, y and z are L, M and N respectively and rotation rates are p, q, and r respectively. The aerodynamic forces are normalised by the base area of the Orion, A_b, and the dynamic pressure, Q. The reference length for moment coefficients is the Orion diameter, d.

6. UQ2 HDT RESULTS

6.1 Source flow Correction

Force data were reduced using dynamic pressure at the model's centre of pressure. This minimises the effect of the 17% reduction in Q over the length of the model produced by the diverging flow of the conical nozzle. Centre of pressure, measured from the base, was reduced by $0.32d$ to compensate for the lower Q at the tail in comparison to that at the nose. The correction was derived by noting that the normal force is primarily comprised of two components: F_1 at the nose, a distance $x_1 \approx 4.6d$ from the centre of pressure; and F_2 at the tail, a distance $x_2 \approx 4.6d$. Thus the shift in centre of pressure due to a c%/m decrease in dynamic pressure is approximately,

$$\Delta x_{cp} \approx \frac{c(x_1+x_2)F_2x_2}{100(F_1+F_2)} = \frac{c}{100}x_1x_2 \qquad (1)$$
$$= \frac{.015}{d}\times 4.6d \times 4.6d = 0.32d$$

6.2 Aerodynamic coefficients

Axial force C_x, Normal force, C_z, and Pitching moment, C_m are plotted in figure 6. Pitching moment is taken about the UQ-Orion centre of gravity, $5.89d$ from the base.

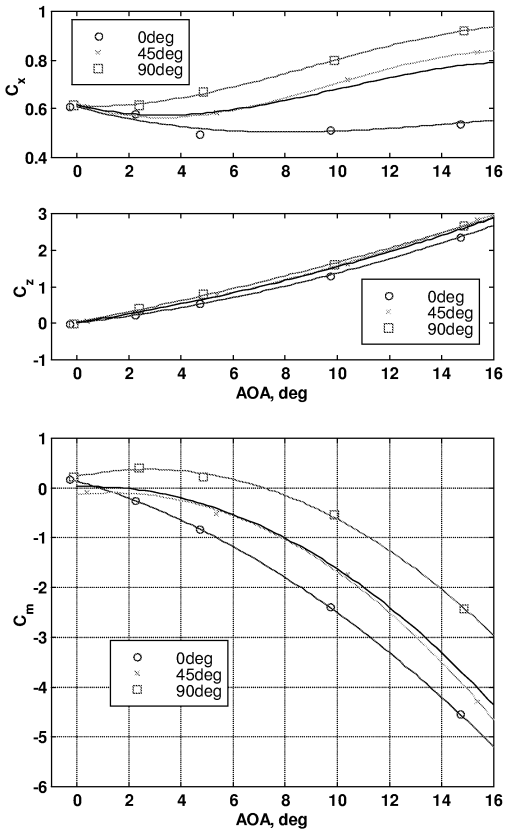

Figure 6 Measured aerodynamic coefficients

Least-squares curve-fits are plotted as continuous lines with the data in the figures. The black line that closely follows the 45° roll result, is a curve fit to the roll averaged values that are obtained by assuming linear

variation of the coefficients from 0° to 45° and 45° to 90°. For example, the roll averaged value of C_z is,

$$\overline{C}_z = \frac{C_z(0°)}{4} + \frac{C_z(45^\circ)}{2} + \frac{C_z(90°)}{4} \qquad (2)$$

The trajectory calculation was based on the curve fits to the roll averaged coefficients in table 2. Non-roll-averaged coefficients (including C_y and C_n) may be necessary to improve prediction at low altitude as discussed later.

Source	Coeff.	σ^3	σ^2 or $\sin^2\sigma$	σ or $\sin\sigma$	1
HDT	C_x	-31.4	16.7	-1.56	0.62
σ<16	C_z		14.3	6.27	0.02
	C_m		-59.6	-0.9	0.03
Newt.	C_{mq}		-2003	-45.6	-118
σ<16	C_{nr}		24.7	-144	-113
Newt.	C_x		-0.14	0.39	0.32
σ>16	C_z		27.1	1.78	-0.03
	C_m		-75.5	7.35	-0.06
	C_{mq}		254	-1073	1.2
	C_{nr}		37.2	-156	-110
FM	C_x		-4.50	12.8	2.14
σ<16	C_z		23.6	6.13	0
	C_m		-66.7	-11.3	0
FM	C_x		-12.2	18.6	1.04
σ>16	C_z		25.3	5.07	0.17
	C_m		-56.6	-18.0	1.13

Table 2 Polynomial coefficients for the aerodynamic data. Sinσ is used to fit C_z and C_m from the Newtonian and Free molecular calculations. All other polynomials are for σ in radians.

7. HIGH ANGLE OF ATTACK AERODYNAMICS AND DAMPING

Newtonian and free molecular theory were used to estimate the aerodynamics of the vehicles at angles of attack greater than 16°. The UQ-Orion body was approximated as a cone-cylinder-cone-cylinder defined by the (x, r) non-dimensional co-ordinates [(0, 0) (1.21, 0.39) (1.92, 0.39) (2.06, 0.5) (11.2, 0.5)]. The fins were modelled as flat plates. Fin forces were taken as the highest of the Newtonian and linear theory estimates, the crossover to Newtonian occurs when angle-of-attack exceeds 18°. Figure 7 shows the calculated coefficients and for comparison the measured roll-averaged-coefficients.

Newtonian theory was also used to estimate the "dynamic derivatives". The damping mechanism is simple: the component of flow velocity normal to the vehicles surface is decreased by the vehicle's rotation at positions ahead of the centre of gravity and increased behind. This modification to the surface pressure produces a moment that acts to retard the rotation. As for the static coefficients, Linear theory was used to estimate the fin forces at small angles of attack. In this case damping results from the rotation rate producing an effective angle of attack at the fin, with the resulting Lift-generated-moment opposing the rotation. Free molecular values were not calculated since the effect of damping is negligible at high altitude (dynamic pressure and pitching rates are both too low).

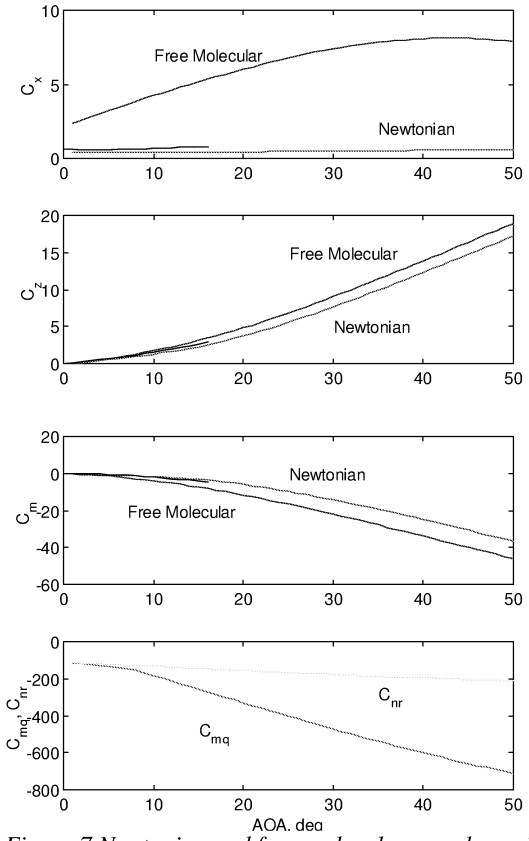

Figure 7 Newtonian and free-molecular aerodynamic coefficients. Measured roll-averaged values are in black.

Even with axisymmetric bodies damping in yaw is generally not the same as that in pitch at non-zero angle of attack. To avoid cross coupling (e.g. rotation about the z axis causing a moment about the y axis) it is necessary to calculate the damping moments in wind axes. Using the wind tunnel axes system previously described, the pitch-damping derivative is C_{mq} and the yaw-damping derivative is C_{nr}. The derivatives are defined with British convention as,

$$C_{mq} = \frac{M_{cg}}{(qA_b)d}\frac{V}{qd} \qquad C_{nr} = \frac{N_{cg}}{(qA_b)d}\frac{V}{rd} \qquad (3)$$

The calculated dynamic derivatives are plotted in figure 7. Note the large difference between the pitch and yaw values. This is primarily due to the contribution of the fins which are effectively oscillating about zero incidence in yaw but are more active in pitch as incidence increases.

8. HIGH ALTITUDE AERODYNAMICS

High altitude aerodynamic coefficients were obtained in the conventional manner by "bridging" the Newtonian and free molecular values with an equation of the form,

$$C(M,Re) = C_{Newt} + f(M,Re) \times \left(C_{fm} - C_{Newt}\right) \qquad (4)$$

where: the bridging function f ranges from 0 to 1 as Re decreases from ∞ to 0, and was determined empirically from the LDT data.

For axial force coefficients the function,

$$f = \frac{M/\sqrt{\mathrm{Re}}}{0.5 + M/\sqrt{\mathrm{Re}}} \qquad (5)$$

is well known to fit many low density tunnel data while having the correct form to describe laminar shear stress contributions at low altitude. The LDT data for UQ1 at a Knudsen number of 0.006 supported this function for C_x but C_z and C_m were close to the free molecular value. This suggested a much earlier transition was appropriate. For C_m and C_z we used the function,

$$f = \frac{Kn}{0.002 + Kn} \qquad (6)$$

Figure 8 shows the chosen bridging functions as a function of altitude assuming descent at a constant Mach number of 7.6. The bridge for moment and normal force has the desired properties of a rapid and early transition to the free molecular level but at low altitude it does not introduce an artificial Reynolds number effect on the force and moment. The points corresponding to HDT and LDT conditions are marked on the bridging functions.

Aerodynamics for σ<16° were based on the HDT data and free molecular values using the same bridges in equations of the form,

$$C(M,Re) = C_{HDT} + \frac{f(M,Re) - f_{HDT}}{1 - f_{HDT}}\left(C_{fm} - C_{HDT}\right) \qquad (7)$$

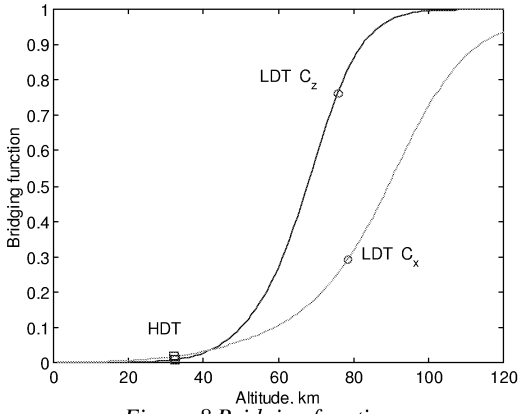

Figure 8 Bridging functions

9. COMPARISON WITH FLIGHT

A six degree of freedom trajectory code was used to calculate the UQ-Orion motion during re-entry. Initial conditions were determined as described by (Owen and Cain, 2004). Mass properties and aerodynamic coefficients were as defined in figure 2 and table 2 respectively. Roll torque coefficients were estimated to be C_L=0.02 and C_{Lp}=-1.2 by matching the spin, p, deduced from the magnetometer output, figure 9. The sudden reduction in p that occurs at 542s was not modelled and is possibly a sign of fin failure.

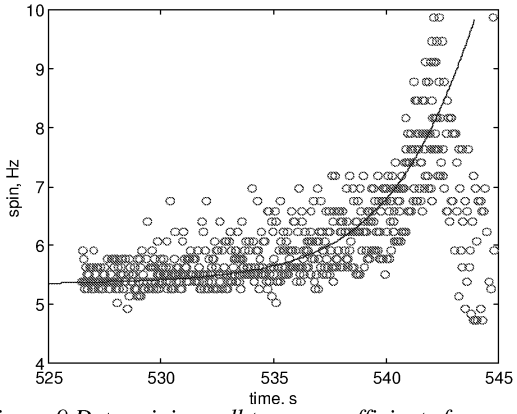

Figure 9 Determining roll torque coefficients from spin

Predicted pitch, θ, and x magnetometer output are plotted along with the flight data in figure 10. The departure from sinusoidal motion at 515s corresponds to the UQ-Orion entering the atmosphere. The reasonable agreement in frequency, magnitude and phase of the oscillations is a sign that the predicted pitching moments and adopted mass properties are close to actual. The angle of attack, σ, is also close to the value inferred from the intake measurements (Owen and Cain, 2004) but the decay rate of the mean σ is higher than predicted, and the decay rate of the oscillations in σ is lower than predicted.

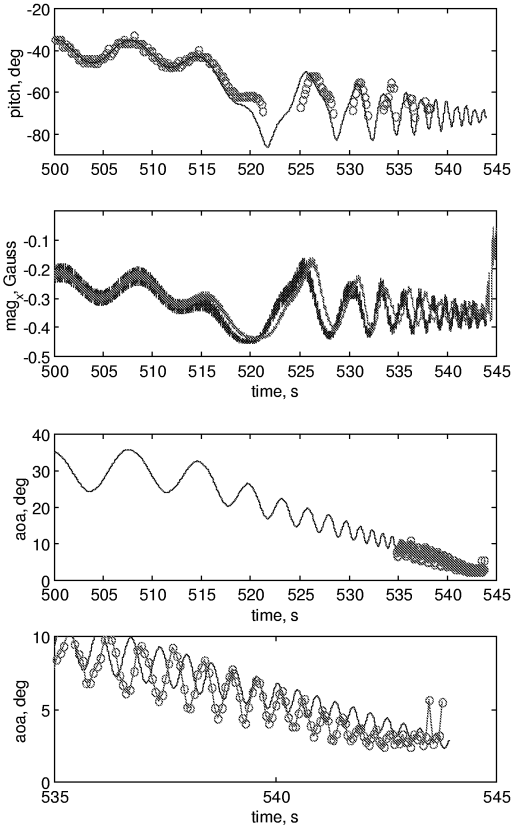

Figure 10 Comparison of simulation with flight data

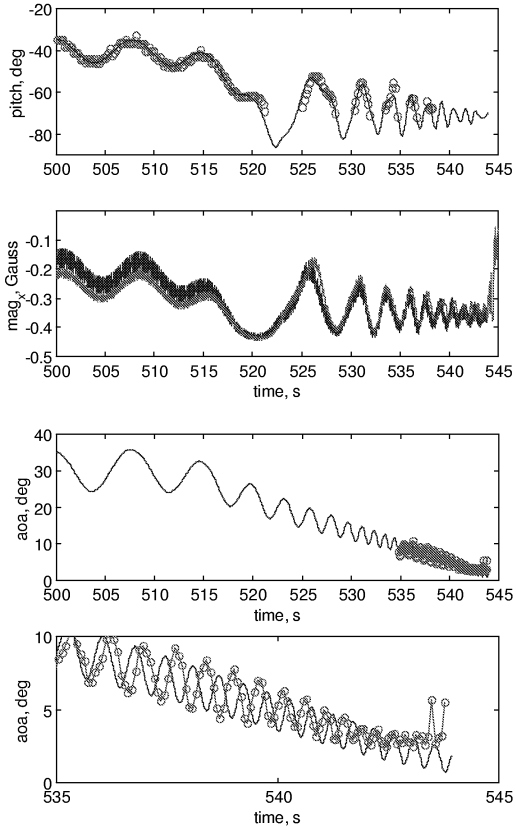

Figure 11 Comparison of simulation with flight data using the modifications described in the text

The UQ-Orion exhibits classical angle of attack behaviour of a spinning body, which for small σ can be modelled analyically as the sum of two rotating vectors. The "nutation arm" that rotates in the direction of the spin at frequency ω_1 and the "precession arm" that rotates in the opposite direction at frequency $-\omega_2$. The sum of the frequencies, $\omega_1+\omega_2$, is equal to the free space nutation frequency and the product $\omega_1\omega_2$ is equal to the square of the weathercock frequency. The decay rate of the mean σ (the precession arm) is set by C_{nr} and that of the oscillations (the nutation arm) set by C_{mq}. The initial nutation arm length is the angle between the vehicle axis and its angular-momentum-vector (the coning angle prior to re-entry). The initial precession arm length is the angle between the velocity vector and angular momentum vector.

Some relatively minor adjustments can improve the simulation. Figure 11 is a repeat of figure 10 with the initial yaw angle reduced by 14°. C_{mq} has also been set to zero and C_{nr} increased by a factor of three. At lower altitudes where ω_1 would become comparable to the spin frequency p, further improvement might result from using non-roll-averaged values of the aerodynamic coefficients.

10. CONCLUSIONS

The data from the Hyshot-2 flight provided a valuable check on the techniques and wind tunnel data used to model hypersonic atmospheric re-entry. The agreement was in general very good but our calculations of aerodynamic damping seem to be in error with C_{mq} overestimated and C_{nr} underestimated.

11. ACKOWLEDGEMENT

This work was carried out as part of the Weapon and Platform Effectors Domain of the MoD Research Programme. The authors would also like to thank Prof. Allan Paull at the University of Queensland for providing the flight data.

12. REFERENCES

Owen R and Cain T., *Reconstruction of the Hyshot2 flight from onboard sensors,* 5th European Symposium on Aerothermodynamics for Space Vehicles, Cologne, Germany, 8-11 Nov., 2004.